Some insights on theoretical reaction dynamics: Use of absorbing potentials and exact three-dimensional calculations.

Fermín Huarte Larrañaga

Some insights on theoretical reaction dynamics: use of absorbing potentials and exact three–dimensional calculations

Fermín Huarte Larrañaga
Departament de Química Física
Universitat de Barcelona

UNIVERSITAT DE BARCELONA

Chapter 9

Exact Hyperspherical calculations.

Contents

9.1 Exact quantum 3D cross sections for the $Ne + H_2^+ \rightarrow NeH^+ + H$ reaction by the hyperspherical method. Comparison with approximate quantum mechanical and classical results.

Physical Chemistry Chemical Physics 1 (1999) 1125-1132

In this article we published our first results on the exact quantum mechanical study on the $Ne + H_2^+ \rightarrow NeH^+ + H$ reactive system using the hyperspherical method as described in section 5.1. The relatively recent technological development as well as the appearance of the first practical numerical codes has given new impulse to the exact quantum mechanical computation of reactive scattering. However, still few methods have proven to be capable of performing such calculations under reasonable bounds of computational resources. One of the most powerful and widely used is that developed by Launay and LeDorneuf, which we have employed in the works described here.

In particular we have studied a member of the series $X + H_2^+$ reactions, where $X = He, Ne, Ar$, for which a considerable amount of experimental data is available. Besides, the $Ne + H_2^+ \rightarrow NeH^+ + H$ reaction is commonly found in the field of plasma physics, where atoms of Ne are introduced into H_2 plasma to act as a cooling H_2^+-quenching system. Two outstanding features make this reaction worth studying. These are the significant reactivity enhancement caused by vibrational excitation and, mainly, the structured shape of the reaction probability plotted as a function of energy, which could be revealing of a dense scattering resonance spectrum. We had already at hand previously published preliminary results that were useful in the seek of convergence parameters, a rather critical feature in any numerical calculation.

In the following article, a quite careful description is given on the search for optimum convergence parameters. The reason for this is the system's sensitivity to small variations of the main parameters. Thus, the convergence process was checked on the $J = 0$ reaction probability using not a small set of energies but a whole set of closely spaced energies, around 800 energy values within a 0.4 eV range. The main parameters converged were the maximum (asymptotic) value of the hyperradius, the number of sectors, number of meshpoints in each sectors and the size of the internal basis. In particular, special attention was payed to the ρ_{max} convergence and our results confirmed those previously published. Next, convergence conditions were established for the complete integral cross section calculation, in particular the value of the last contributing total angular momentum and the number of J projections that has to be included in the propagation.

Results obtained confirm the significantly higher effectivity of the vibrational energy mode. The remarkable resonant structure seems to be caused by long lived compound states rather than by some centrifugal barrier effect. Our exact results were extensively compared with several other approximate methods such as CS, R-IOS and QCT giving different levels of agreement. The QCT results were unexpectedly wrong, probably due to a systematic violation of the ZPE conservation rule, while the CS were the closest ones to the exact.

PCCP

Exact quantum 3D cross sections for the $Ne + H_2^+ \rightarrow NeH^+ + H$ reaction by the hyperspherical method. Comparison with approximate quantum mechanical and classical results

Fermín Huarte-Larrañaga,[a] Xavier Giménez,[a] Josep M. Lucas,[a] Antonio Aguilar[a] and Jean-Michel Launay[b]

[a] *Departament de Química Física, Universitat de Barcelona, Martí i Franquès, 1. 08028 Barcelona, Spain*
[b] *PALMS, UMR 6627 du CNRS. Université de Rennes 1, Campus de Beaulieu, 35042 Rennes Cedex, France*

Received 3rd November 1998, Accepted 14th December 1998

Exact, fully converged three-dimensional quantum mechanical cross sections for the title reaction have been computed on the analytical potential energy surface of Pendergast, Heck, Hayes and Jaquet. The close-coupling hyperspherical method of Launay and LeDourneuf has been used for the calculations. Results explicitly shown here correspond to reaction probabilities as a function of total energy and J, integral cross sections and product rotational distributions, for the first three reactant vibrational levels and the ground $j = 0$ reactant rotational level. Integral cross sections confirm the main experimental findings: (a) vibrational excitation greatly enhances reactivity and (b) the reactivity threshold is near the opening of the $v = 2$ reactant channel. Product rotational distributions show an unimodal shape, with its maximum lying at intermediate values of the open product rotational quantum numbers. Results have been compared with previously available centrifugal sudden (CS) and reactive infinite order sudden (R-IOS) results, as well as with quasiclassical trajectory (QCT) calculations. As a general trend, CS and R-IOS integral cross sections show the same qualitative shape as the exact ones, the CS ones being very close to exact but those of R-IOS are between four and five times lower. The QCT results are three times lower and fail to reproduce the threshold behaviour. CS rotational distributions are slightly hotter than exact ones, while QCT results are closer to the exact ones except for the fact that they populate rotational levels not allowed when considering both the zero-point energy and the total energy conservation.

1 Introduction

The exact quantum mechanical computation of dynamical properties—*i.e.* from state-to-state reaction probabilities to thermally averaged rate constants—for elementary chemical reactions is an emerging field of theoretical chemistry.[1] It proves necessary, among other reasons, for (a) comparing with experimental information and then refining the potential energy surface, (b) establishing the accuracy of approximate scattering methods and (c) developing new accurate methods. All these items have been the subject of considerable effort in recent years.[2] For the above purposes, of special interest is the computation of those dynamical quantities such as state-to-state and state-to-all integral cross sections which, although being averaged, are still directly comparable with experiments while being sensitive enough to the details of the potential energy surface. However, very few methods have been shown to be capable of performing these calculations while keeping within reasonable bounds the use of computational resources. Among these, the close-coupling hyperspherical method as developed by Launay and LeDourneuf[3] is one of the most powerful and extensively used since it has been able to produce reactive cross sections for the $H + H_2$,[3] $F + H_2$,[4] $F + D_2$,[5] $He + H_2^+$,[6a,b] $Cl + H_2$ (ref. 7) and $H + HCl$ (ref. 8) systems.

In the present work, the above methodology has been applied to the study of the $Ne + H_2^+ \rightarrow NeH^+ + H$ reaction. It belongs to the $(X + H_2^+)$ family of reactions (X = He, Ne, Ar), which were studied in numerous high-quality experiments, yielding data that ranged from temperature-dependent rate constants to differential cross sections.[9–15] In addition, processes involving the title reaction are also of great importance for practical purposes, mainly for plasma physics. For instance, adding Ne atoms to hydrogen plasma systems causes a significant cooling close to the walls, since Ne atoms efficiently quench the highly excited H_2^+ ions.[16]

Rather refined fits to potential energy surfaces are available for the title reaction that can be used to compare theoretical approaches and experimental results.[17–22] Several works focused on the theoretical simulation of the reaction dynamics, covering from collinear to approximate three-dimensional quantum methods as well as collinear to three-dimensional quasiclassical trajectory calculations.[17–28] These studies served both as a tool for a dynamical testing of the potential energy surface and as a means for obtaining the main trends of the reaction dynamics. Of special relevance for the present study is the work of Kress, Walker, Hayes and Pendergast (hereafter denoted as KWHP),[25] who reported exact 3D probabilities for zero total angular momentum (J) at 800 values of the collision energy. Two outstanding features are the effectivity of vibrational excitation in promoting reactivity and the extremely structured shape of the reaction probability as a function of energy. The latter reveals the existence of a dense spectrum of scattering resonances. A more complete

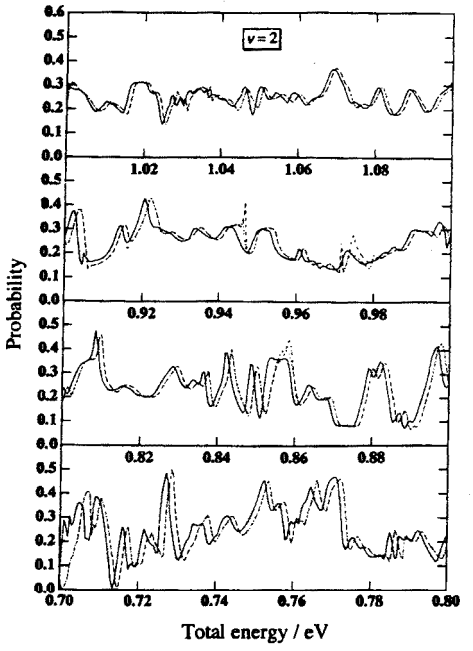

Fig. 1 Comparison between KWHP (see text) $J = 0$ reaction probabilities[25] as a function of total energy, for the reactants vibrational state $v = 2$ and ground reactants rotational state, and the same, present, results obtained with several numerical parameter sets. (——) KWHP results. (····) present results with matching distance, $\rho = 13$ a_0, number of surface functions, $N = 120$, number of mesh points within a sector, NMSH = 5, number of internal basis functions, NB = 55, number of sectors, NS = 110. (----) $\rho = 13$ a_0, $N = 120$, NMSH = 5, NB = 90, NS = 110. (– – –) $\rho = 13$ a_0, $N = 120$, NMSH = 5, NB = 55, NS = 139. Higher values of N, NMSH, NB and NS were tested and were, graphically, indistinguishable from those shown here. See Fig. 2 for results corresponding to the ρ-convergence test.

study of the reaction cross section was then performed by Gilibert *et al.*,[29] calculating state-selected integral cross sections as a function of energy, through the use of the coupled states approximation. The $J = 0$ reaction probabilities are in agreement with KWHP, although some discrepancies were found which will be discussed later. Integral cross sections showed a most remarkable structure in their dependence *versus* energy, indicating the survival of reactive scattering resonances within the centrifugal sudden (CS) approximation.

The experience gained with the existing theoretical studies indicates that these systems, more than other known triatomic reactive species, are dominated by strong quantum effects. This conclusion has been extracted from quantum mechanical reduced dimensionality treatments, and the implications concerning the relevance of quantum effects in chemical reaction dynamics are seemingly important. However, the quantitative assessment of the actual importance of quantum effects can only be obtained by means of an exact estimation of the quantum reactivity.

The moderately endoergic—0.50 eV from the electronic reactants to products asymptotes—$Ne + H_2^+ \rightarrow NeH^+ + H$ reaction takes place on the ground $^2A'$ PES of the system. The analytical fit to *ab initio* calculations,[22] here used for the whole set of calculations and methods (which corresponds to the PHHJ3 PES fit of ref 22), reveals a barrierless collinear minimum energy path with a 0.51 eV collinear well in the entrance channel. The reactants zero-point energy (ZPE) is 0.14 eV, while products ZPE is 0.18 eV, so that the endoergicity, considering the ZPE, is 0.54 eV. As the bending Ne—H—H angle is decreased, the potential well is increasingly milder but then a barrier to reaction gradually emerges. The result is that at 60° no vestige of the potential well remains and the reaction barrier is high enough to prevent reaction below 1.5 eV.

The remainder of the paper is organized as follows. Section 2 briefly describes the methodology here used and the detailed tests made to ensure convergency of results. In Section 3, the main results are presented and compared with previously available approximate calculations. Section 4 discusses both how different methods compare and some features of the exact reaction dynamics. Finally, Section 5 concludes.

2 Outline of the method and convergence tests

The method used in the present work is the close-coupling hyperspherical method of Launay and LeDourneuf,[5] which has been described with some detail elsewhere.[3,6] For this reason, only an outline of the practical steps will be given here.

The Hamiltonian of the system is expressed in a modification of the Smith–Whitten democratic hyperspherical coordinates (ρ, $\bar{\omega}$, $\bar{\omega}_E$, body-fixed the axis-dependent internal angles, respectively, which plays the role of the scattering coordinate, $\bar{\omega} = (\theta, \phi)$ the set of polar and azimuthal internal angles, respectively, and $\bar{\omega}_E = (\alpha, \beta, \gamma)$ the set of Euler angles), which transform very simply between arrangement channels. The global wavefunction is expanded in terms of products between the solutions of the internal angle problem and symmetrized Wigner rotation functions that describe the motion associated to the Euler angles. Then, the expansion is substituted into the Schrödinger equation for nuclear motion and the solution of the resulting close-coupling equations is obtained through three steps: a J-independent interaction matrix is constructed first at several previously fixed values of the hyperradius. In a second stage, the J-dependent information, including the Coriolis coupling terms, is calculated and added to the interaction matrix elements. Finally, a third stage propagates the whole set of hyperradial solutions (actually their log-derivative transform) along the hyperradius by means of the Johnson–Manolopoulos invariant embedding propagation method,[30,31] yielding first the reactance K-matrix and then the S-matrix. The squared modulus of the S-matrix elements gives each state-to-state collision probability and, in particular, all reaction probabilities. It is interesting to note that within this partitioning of the Hamiltonian, the first and second stages are solved once and the resulting interaction and transformation matrices stored, while the third stage uses that information as many times as total angular momentum values and collision energies are considered.

A major step in the present calculation has been establishing the optimum convergency conditions. The reason is that, for this system, it has been previously shown that the reactivity is rather sensitive to small variations of the main numerical parameters. For instance, the KWHP study shows that the $J = 0$ reaction probability is strongly structured as a function of energy, so that looking for convergence with only a few probability values may be meaningless. In addition, the same study evidences that reaction probabilities are found to be sensitive to the (rather large) hyperradius value at which the asymptotic matching is made. In this sense, Gilibert *et al.* showed in their first CS study[29] that increasing the propagation range led to a small but significant variation of the reaction probability shape. This variation was initially attributed

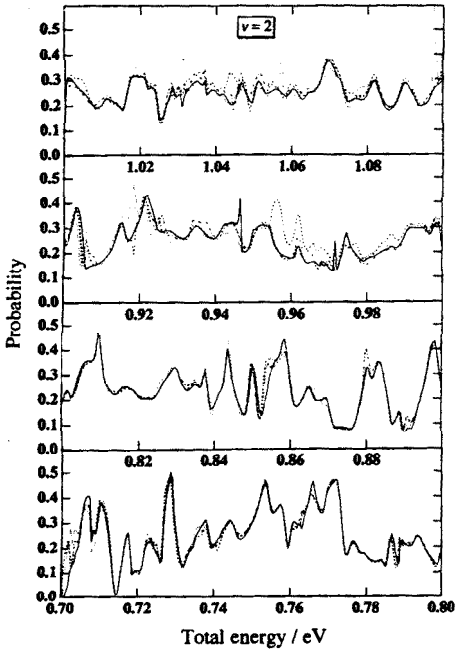

Fig. 2 Asymptotic matching distance convergence test with the $J = 0$ reaction probabilities as a function of total energy. All curves correspond to $N = 120$, NMSH = 5, NB = 55 and NS = 110 (see text of Fig. 1), and: (——) $\rho = 13\ a_0$, (···) $\rho = 14\ a_0$, (-·-·) $\rho = 15\ a_0$ and (– – –) $\rho = 16\ a_0$.

to the rather long range of the potential, owing to the ionic nature of the interaction. A minor lack of convergence was detected afterwards and the CS calculations were remade,[32] showing a better agreement with the exact results at the former matching distance.

Because of that, it was decided that a better display of the convergence process might be obtained by checking the $J = 0$ reaction probability convergence, not with a small set of distant energy values but with a whole set of closely spaced energy values, for each necessary numerical parameters set. An explicit study of the dependence of the reaction probability with the final hyperradius value has been also included. Fig. 1 shows the dependence of the $J = 0$ reaction probability with total energy, for two sets of numerical parameters. Some 800 values of the collision energy have been calculated. These results are compared with the available $J = 0$ KWHP results. Our best curve shows excellent agreement with KWHP, the only difference arising as a small constant energy shift. This kind of disagreement may probably be owing to a minor discrepancy in the conversion from collision into total energy. Other calculations with higher values of the numerical parameters have been performed. They were, graphically, indistinguishable from our best results of Fig. 1.

Thus, the above study has consisted, basically, in establishing the accuracy of the present study at the conditions given by KWHP. Next, given the controversy about the matching hyperradius value, we thought it convenient to go further and check the influence of the propagation range on the reaction probability. Since the calculation of a single $J = 0$ probability result is reasonably cheap, the whole energy set was generated again for each numerical case, so that convergence could be checked more stringently. Fig. 2 shows the

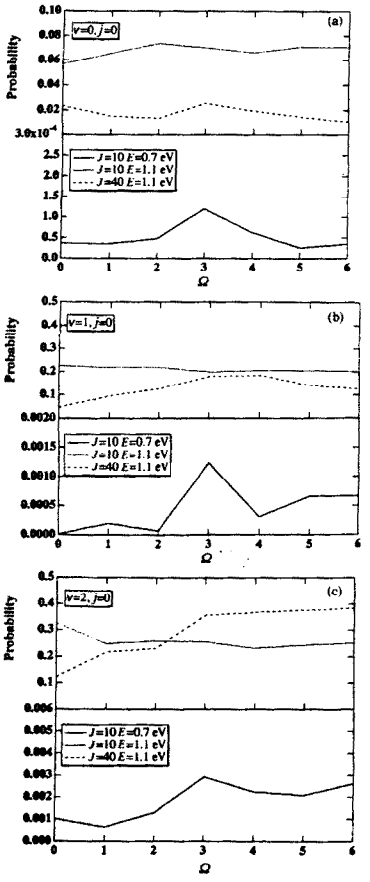

Fig. 3 (a) Dependence of the reaction probabilities on the number of Ω projections included in the close-coupling calculation, for the initial state $v = 0$, $j = 0$. (——) Total angular momentum $J = 10$ and total energy $E_{tot} = 0.7$ eV. (···) $J = 10$ and $E_{tot} = 1.1$ eV. (– – –) $J = 40$ and $E_{tot} = 1.1$ eV. (b) The same as (a). $v = 1$, $j = 0$. (c) The same as (a). $v = 2$, $j = 0$.

$J = 0$ reaction probability, as a function of total energy, at four values of the matching hyperradius. Overall, results are strongly coincident, so that a small to null influence of the propagation range is observed. However, a more detailed inspection reveals that higher—although still reasonably small except for very few energy values—variations are observed in localized regions of the scanned energy range. In view of this, we conclude that, for the purpose of the present study—*i.e.* the computation of integral cross sections and product rotational distributions—these discrepancies are of no relevance and the propagation range has been kept at $\rho = 13\ a_0$. However, for very detailed state-to-state probability studies it might be necessary to increase the value at which the asymptotic matching is performed. The final set of numerical parameters[3,6] were the following: 120 surface functions have been included in the propagation step, which have been built up with the use of 953 primitives and from 30 to 75 internal functions. Propagation runs from 2.1 to 13.0 a_0, including a total of 165 sectors into which the hyperradius has been divided. Within each sector, five mesh points have been used. A basis contraction[3,6] was used at large ρ.

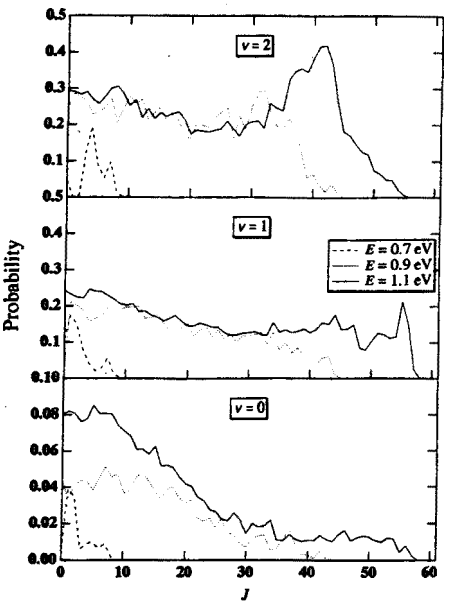

Fig. 4 Reaction probability as a function of the total angular momentum J, for $(v, j) = (0, 0)$ (lower panel), $(v, j) = (1, 0)$ (middle) and $(v, j) = (2, 0)$ (upper). Note the scale change for $v = 0$. (——) $E_{tot} = 1.1$ eV. (····) $E_{tot} = 0.9$ eV. (– – –) $E_{tot} = 0.7$ eV.

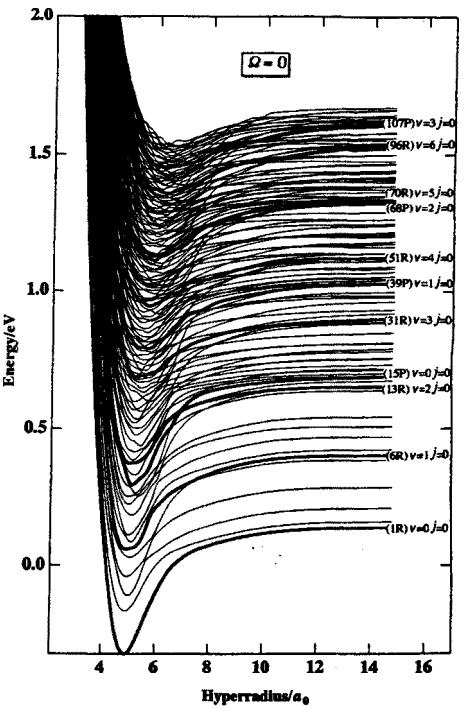

Fig. 5 Adiabatic internal problem eigenvalues as a function of the hyperradius, for $\Omega = 0$. They correlate asymptotically with each reactant or product rovibrational state, which is indicated by its ordering number, followed by a letter stating whether it correlates with a reactant (R) or a product (P) level and, finally, the (v, j) rovibrational asymptotic state.

The following step consisted in establishing the convergence conditions for the complete integral cross section calculation. According to the traditional formulae[2] and the previous experience in exact and CS calculations,[2–8,29,32] the integral cross section must be converged upon adding contributions from successively higher values of J, the total angular momentum, and upon considering successively higher projections of J [illegible] Ω [illegible] quantization axis. Fig. 3(a)–3(c) show the dependence of the reaction probabilities on the number of Ω projections included in the close-coupling calculation, for the three open reactant vibrational states. It is clearly evidenced that for $\Omega \geq 6$ the probabilities should not vary appreciably, so this value has been taken as the maximum projection for the calculations. The total angular momentum range necessary for convergence is easily checked by means of the opacity function, which is shown in Fig. 4. As the energy is increased, the maximum vaue of J, J_{max}, rises, to ensure convergence, from 10 at 0.7 eV to 61 at 1.1 eV. The total computational cost for the generation of the complete set of adiabatic states, for all sectors and Ω values, was *ca.* 133 CPU hours, while the calculation of a single energy cross section took an average of 2 CPU hours. All calculations were performed on a two processor (R8000) Silicon Graphics Power Challenge L Workstation, using up to 400 Mbytes of core memory.

3 Results

Having determined the optimum values of the parameters which control the numerical convergence of results, production runs were undertaken to characterize the exact dynamics of the Ne + H_2^+ system.

Fig. 5 shows the adiabatic internal problem eigenvalues as a function of the hyperradius, for $\Omega = 0$, which correlate asymptotically with each reactant or product rovibrational state, while Fig. 6 shows the corresponding eigenvalues for $\Omega = 6$.

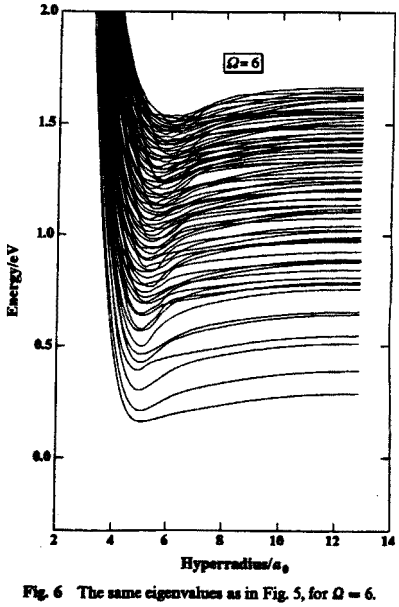

Fig. 6 The same eigenvalues as in Fig. 5, for $\Omega = 6$.

This latter figure has been included to evidence the upwards energy shifting effect of the centrifugal angular momentum term. A more detailed picture of this effect is shown in Fig. 7, which shows how the ground surface function state is specifically influenced by the Ω quantum number. The asymptotic degeneracy shown by the $\Omega = 1$ and 2 curves (and also by $\Omega = 3$ and 4 and by $\Omega = 5$ and 6) is due to nuclear symmetry restrictions to the total wavefunction, which prevent, in the present case, reactants in odd rotational states to exist, since the calculations focus exclusively on the even parity block with respect to nuclei inversion. Because of that, the first $\Omega = 1$, 3 and 5 adiabatic states are forced to correlate with the $v = 0, j = 2$, 4 and 6 H_2^+ asymptotic states, respectively.

The whole set of rovibrational adiabatic curves display a bonding-like form, which is gradually smoothed down as Ω increases. This form of the adiabatic curves clearly reflect the influence of the electronic minimum in the PES. No centrifugal-like barriers are observed, so that resonance trapping, found for the present reaction to occur very frequently as a function of energy, must correspond to complex, Feshbach type. It is interesting to also note that most of the avoided crossings take place before the potential ridge, *i.e.* the region to the left of an imaginary line, starting approximately at 6 a_0 and 0 eV and ending at 8 a_0 and 1.5 eV. This behaviour is of relevance when deciding the ρ-dependence of the effective width and the internal basis dimension, since the most important non-adiabatic couplings between rovibrational states are expected to occur there.

In Fig. 8 the result of the integral cross section calculation is shown, for 31 energies, for the reactants vibrational states $v = 0$, 1 and 2 and for the ground reactants rotational state ($j = 0$). From here on, the $j = 0$ case is assumed. Results corresponding to equivalent CS, QCT and R-IOS calculations are also shown for comparison purposes. The related numerical details can be found elsewhere.[29,32] The main features of the exact results are the following. Although the minimum energy path is barrierless, the excitation function shape is typical of systems having a barrier. This is owing to the interposed barrier emerging for noncollinear configurations. Vibrational excitation clearly promotes reactivity since the vibrational ratio 0 : 1 : 2 (each number being the corresponding reactant vibrational quantum number) is approximately, on average, 1 : 10 : 25. This is also consistent with the delayed position of the transition state. The excitation function shape for $v = 0$ and 1 is qualitatively different from that of $v = 2$. For this latter, the reactivity increases sharply, reaches a maximum at 0.73 eV and then decreases slightly within a low-frequency oscillatory pattern which leads to a smooth final increase. On the contrary, for the former states the reactive cross section increases monotonically within the whole investigated energy range. Finally, a high-frequency structure is present in the excitation function shape, especially for $v = 2$, which is probably owing to the manifestation of reactive scattering resonances at the cross section level. However, its proper characterization will require a much finer energy grid especially for $v = 2$ as its variation with energy is rather sharp.

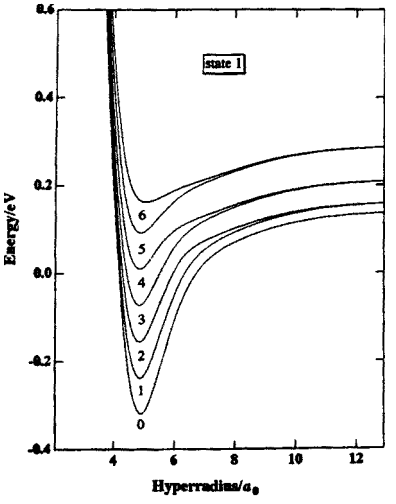

Fig. 7 The ground adiabatic internal problem eigenvalue, as a function of the hyperradius, for $\Omega = 0$–6.

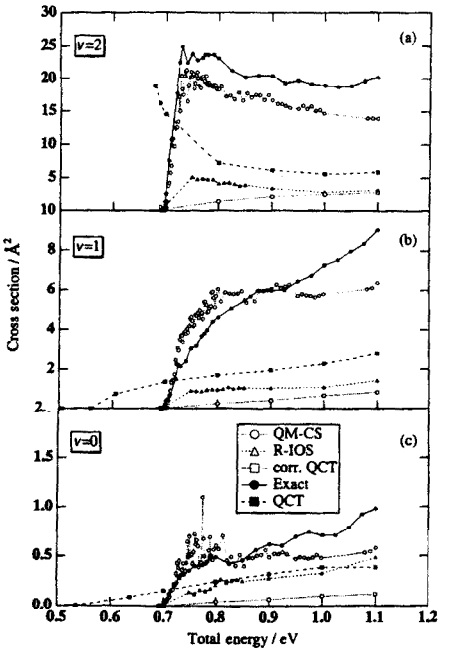

Fig. 8 Total integral reaction cross section as a function of total energy for $v = 0$ (c), $v = 1$ (b) and $v = 2$ (a), for the ground reactants rotational state. Note the scale change when going from $v = 0$ to $v = 2$. (●) Present exact results; (○) CS results; (■) QCT results; (△) R-IOS results; (□) corrected-QCT results (see text).

The exact integral cross sections are, overall, the highest when compared with those calculated by means of the approximate methods here used (although the BCRLM cross sections computed by KWHP, on the same surface, are a fair way above the exact ones, a tendency which was also obtained in an equivalent comparison for the He + H_2^+ system[6]). This means that the approximated terms in the Hamiltonian lead to a positive reactive contribution when accounted for exactly. CS results are rather close to the exact ones, although for $v = 0$ and 1 it is found that they lie a bit above at low energies but slightly below at higher energies. For $v = 2$, on the other hand, the CS results are always lower than exact. Remarkably, the much discussed oscillatory pattern of the $v = 2$ exact results is also reproduced by the CS calculations. The structured behaviour of the CS integral cross section is more intense than the exact one, especially for $v = 0$.

R-IOS results are about five to four times lower than exact ones, except for $v = 0$ which are closer to the exact calculations (two times lower). On the other hand, the behaviour shown by QCT is more involved. The $v = 0$ results are two times lower than the exact ones and the threshold energy is much lower. The threshold problem is also present for $v = 1$, but in this case reactivity is about three times lower. Finally, for $v = 2$ the reactivity at high energies is almost four times lower and the threshold reactivity goes in the opposite direction to the exact results, leading to an increase that is typical of barrierless reactions. The QCT threshold features are clearly explained in terms of the endothermic nature of the reaction, which leads to a critical influence of the inability for QCT to correctly handle the products ZPE. In the present case, it is manifest in a large number of trajectories ending below the ZPE. The differences in the higher energy, "plateau" reactivity regime are essentially due to quantum effects and will be analyzed later.

The time-independent scattering methods here used, as well as the QCT method, allow for a complete state-to-state study of the reaction dynamics. This points us towards quantities such as product energy distributions. However, owing to the endothermicity of the reaction and the energy range considered, only one—or two at the highest energies here scanned—product vibrational levels are open, so that very little information can be extracted from the product vibrational distributions. For this reason, we have concentrated on the rotational distributions to analyze some aspects of the state-to-state dynamics. Fig. 9 shows the product rotational distributions (PRD) for total energies 0.8 and 1.1 eV and initial vibrational levels $v = 0$, 1 and 2, for the exact, CS and QCT cases (the R-IOS method does not give rotational state-specific information).

Overall, PRDs obtained by the exact, CS and QCT methods show a unimodal distribution, peaking at intermediate values of the open product rotational quantum numbers. They are found to be much more sensitive to translational than to vibrational initial energy. Exact PRDs at 0.8 eV show similar qualitative trends when changing the vibrational energy, the main diference being to shift the distribution maximum from $j' = 3$ for $v = 0$ to $j' = 2$ for $v = 2$. The maximum value attainable is $j' = 7$, owing to total energy conservation. A much wider PRD is observed for $E_{tot} = 1.1$ eV, being the sequence of maxima $j' = 5$, 4, 3 for $v = 0$, 1, 2, respectively. The maximum j' value (14) is again limited by energy considerations. PRDs obtained from CS calculations also show a small influence owing to initial vibration.

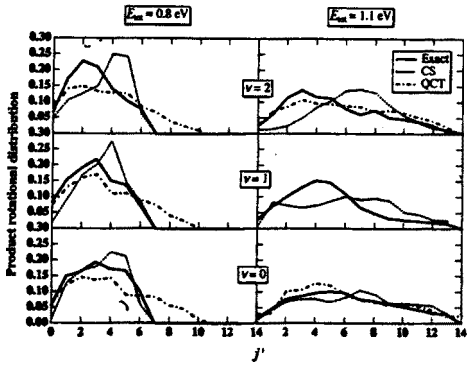

Fig. 9 Product rotational distributions at $E_{tot} = 0.8$ and 1.1 eV and for $v = 0$, 1 and 2 and $j = 0$. (—) Present exact results; (····) CS results; (– – –) QCT results. QCT results for $v = 1$ and $E_{tot} = 1.1$ eV are not available.

However, CS PRDs are hotter than exact ones since they peak at $j' = 4$ for all vibrational levels and $E_{tot} = 0.8$ eV. For the highest total energy CS PRDs are also hotter (peaks are found at $j' = 7$, 6 and 7) although the general trend is closer to exact PRDs than in the low energy case. Finally, QCT PRDs are rather close to exact results (in agreement with previous results for the $H + H_2$ and $F + H_2$ systems[33]), except for a queue which populates $j' \geqslant 7$ at $E_{tot} = 0.8$ eV. This feature arises as a consequence of the violation of the ZPE conservation rule. More specifically, since an important fraction of the computed trajectories end below the products ZPE, more energy than is physically possible is available to be allocated in the remaining modes (rotation and translation).

4 Discussion

As pointed out previously, the late character of the barrier causes the corresponding cross sections to jump by a factor of 25 from $v = 0$ to $v = 2$, although this factor varies with collision energy. This behaviour is in qualitative agreement with the different experimental results,[9] which claim that vibrational levels $v \geqslant 2$ play a major role in determining the reactivity for this system. The threshold position agrees with experimental data,[10] showing that the reaction threshold falls near the $v = 2$ level of the reactant H_2^+ molecule. The decreasing trend of the $v = 2$ reaction cross section is also shown by some experiments.[14] However, in view of the remaining available experimental information, finer refinements of the PES should wait for more precise experimental data.

We will address next the comparison between the results corresponding to the different methods used in the present work. As a general remark, it is important to point out first that comparisons, for the present system, between different methods are rather demanding, since the reactivity shows a marked sensitivity with collision energy. Thus, in addition to the differences attributable to the approximations introduced, quantum effects are so important that discrepancies may appear overemphasized.

The CS calculations show a better overall agreement with exact ones. As far as the accuracy of the CS approximation is concerned, several studies using this approximation are available in the literature.[34] However, owing to the difficulties in having available exact results, very few comparisons between exact close-coupling and CS results have been performed. The first estimations on $H + H_2$ claimed an error of about 25%[35] for the CS method, but the present study, in agreement with other recent ones also performed on heavy systems,[34] points towards a better, even satisfactory accuracy. This also seems to be the rule for tetraatomic systems.[36] As stated above, a remarka e fact is t at t e qual tative trend of the excitation function is strictly reproduced, including the smooth oscillatory pattern obtained between 0.75 and 1.1 eV for $v = 2$. The stronger structure found in the CS cross sections, most probably indicating the survival of resonances at the cross section level, is found to be somewhat quenched in the exact $v = 0$ and 1 cross sections. Nevertheless, the exact $v = 2$ cross section seems to indicate that a marked structure might survive, once a finer grid of results are available, the angular momentum averaging, thus confirming the previous CS findings.

In the present case, the differences between exact and CS results are mainly (a) the exact results show, in the high energy regime, an increasing trend, for all initial vibrational states, which is not so intensively reproduced by the CS method; (b) CS reactivit is shifted downwards about 20% for the whole energy range, for $v = 2$; and (c) CS cross sections, for $v = 0$ and 1, are closer to the exact than for $v = 2$, although they are slightly higher at low energies and slightly lower at high energies. Statements (b) and (c) seem to point out that, overall, an

increase in translational energy makes—as one goes from $v = 2$ to $v = 1$ and $v = 0$ at the same total energy—the CS to lie closer to the exact. This can be expected on the basis that the constancy of orbital angular momentum during the collision event holds better as the translational energy is higher.

The R-IOS results are, as previously estimated for several triatomic reactions,[26,37–41] between one half and one fifth of the exact cross sections. Discrepancies, as it is well known, arise as a consequence of neglecting the reorientation during the approach of the attacking atom towards the diatomic molecule, since it has the effect of forcing the collisions along paths having higher barriers than the ones which would result through reorientation. For this reason, the anisotropy of the potential energy surface plays a main role in establishing the accuracy of the R-IOS method. The present system shows a rather varying bending potential, so that results clearly differ from the non-approximated ones. However, it is found that the qualitative features of the excitation function shape are well reproduced. This leads to the conclusion that relative quantities, such as product vibrational distributions or branching ratios, should work well. In addition, it is also found that an increase in translational energy makes the fixed-angle assumption a better description of the collision picture. This fact explains why the $v = 0$ R-IOS integral cross sections are closer to the exact results.

Rather unexpectedly, QCT cross sections differ very much from the present quantum results. Previous experience indicates that averaged quantities are usually well reproduced by the quasiclassical trajectory method,[33] thus providing a reliable and computationally cheap (as far as core memory is concerned) procedure for characterizing the general trends of the dynamics of an elementary chemical reaction. However, the title reaction is dominated by a pure quantum phenomenon, resonances, whose approximate classical counterpart, the quasiperiodic orbits,[42] do not show the same enhancing effect in reactivity as quantum resonances do.

Perhaps the main difference between both sets of data is the shape and magnitude of the cross sections near the threshold. In all three initial vibrational states it is found that classical results lie very much higher than quantum ones. As stated above, this effect is owing to the well-known limitation of the QCT method regarding the ZPE, which is shown to be crucial in this endothermic barrierless reaction. In the present QCT program,[43] a binning algorithm[44] is used for partitioning the different energy modes. According to this method, rotational and vibrational product energies are assigned to the (v, j) product states which fall nearest, making all necessary corrections to preserve energy conservation. As a consequence, all those trajectories ending below $v = 0$ will be assigned to the $v = 0$ product level. Several corrective procedures have been proposed for the ZPE problem.[45] Despite this, no authoritative answer has been given as to how to correct this problem in a definite and routine way. For instance, simply leaving out these unphysical trajectories may destroy the uniform distribution of phase space states, necessary to obtain statistically meaningful results, while recalculating each failed trajectory with different conditions poses similar problems. Therefore, the easiest approach has been adopted, that is, all trajectories happening with final vibrational energy below that of $v = 0$ are left out. Cross sections are subsequently recalculated for all energies with only those trajectories that meet the physical requirements of the problem.

The result of this correction is shown in Fig. 8 as the corrected-QCT trace. A strikingly large number of trajectories that end below $v' = 0$ is actually found over the whole energy range considered. This causes the excitation function shape to change dramatically as compared with the uncorrected QCT values. The new curves fall systematically far below the quantum results. However, the quantum and classical thresholds to reaction fall by the same energy. The sharpest change in trend is found for $v = 2$, for which the declining shape of the excitation function gives way to a corrected shape that is very similar to the quantum one.

Beyond the threshold region, the difference in magnitude between the quantum and classical results, with the latter falling systematically below the former, must be traced down to the strong non-classical component of the reactive behaviour of this system. Thus, it is found that exact cross sections are up to three times higher than the uncorrected QCT results for $v = 1$ and 2. For $v = 0$, the ZPE problem causes the uncorrected QCT cross sections to be roughly half of the exact ones. Although one may expect that the difference between classical and quantum results might be smaller as energy is increased, for the present system it is shown that, within the scanned energy range, this tendency is not observed. Inspection of the exact and QCT opacity functions (the latter being shown in detail in ref. 32) reveals that high-energy discrepancies are owing both to a difference in reaction probability (*ca.* 0.3 for the exact $v = 2$, $E = 1.1$ eV but *ca.* 0.2 for QCT) and also to a different angular momentum range ($J_{max} = 61$ for exact but 45 for QCT). This points towards the fact that resonance formation is the collision mechanism responsible for a large fraction of the resulting cross sections, even at high collision energies. In addition, the fact that R-IOS cross sections are much closer to QCT than to exact and CS indicates that the motion associated with the bending modes leads to an important contribution of the overall reactivity. It contributes to the background, non-resonant reactivity, as evidenced by the difference between R-IOS and QCT, and also to the resonant reactivity, as shown by the difference between QCT and exact.

Finally, a last comment will be addressed to the high-frequency structure of the cross section. Previous exact calculations of integral cross sections of the $He + H_2^+$ system[6b] revealed that resonances, for this kind of systems, may survive the angular momentum summation. However, this study also showed that the structure is not so strong so as to allow for experimental detection. The present study seems to show a more marked structure. For instance, the 0.73 eV, $v = 2$ peak seems adequate enough to deserve experimental detection, as shown by the sensitivity and energy resolution of recent experiments.[46] From the theoretical side, this subject has been explored in depth by Schatz, Sokolovski and Connor.[47] Their main conclusion is that, assuming the J-shifting approximation[48] to hold and that the resonances are broad enough (short lifetimes), resonances manifest at the cross section level as a step-like curve rather than a peak. In the present case, however, both assumptions may be too severe since: (a) the J-shifting approximation neglects the influence of the different Ω projections for each J value, while Fig. 3(a)–3(c) show that they actually influence the reactivity for the present system; (b) it is difficult to establish the best rotor geometry for this barrierless, complex-forming reaction; and (c) the electronic minimum leads to stabilized quasibound states so that lifetimes are rather long (and widths small). The detailed importance of resonance formation on the reactivity of the system will be analyzed in a future publication.

5 Conclusions

Exact, fully converged integral reaction cross sections and product rotational distributions have been produced for the title reaction, for the first time. All J values that non-negligibly contribute to reactivity have been included in the calculation, which benefited from the fact that only the projections with $\Omega \leqslant 6$ are actually relevant. Despite the rather long range of the interaction potential, it has been found that a further extension of the propagation range, with respect to previous $J = 0$ calculations, does not lead to significantly different results as far as integral cross sections are concerned. The

general results confirm the enhancing role of vibration and the reactivity threshold near the reactants $v = 2$ opening. Given the fact that the calculations were, in the end, feasible and that the PES for this reaction has remarkable features, it can be stated that, nowadays, exact calculations of integral cross sections are possible on moderately involved triatomic systems.

The exact results have been extensively compared with several other approximate methods, to enable their accuracy, for the present system, to be assessed. The CS results are found to be the closest to the exact ones, being nearer as the translational energy is increased. Detailed qualitative features of the exact $v = 2$ excitation function are also reproduced by the CS method, namely a smooth oscillatory pattern from 0.75 to 1.1 eV. The stronger structure, attributable to resonances, is somewhat quenched when going from CS to exact, although reminiscent enough to merit a further detailed exploration both experimental and theoretically. CS product rotational distributions are slightly hotter than the exact ones. The R-IOS results are between a half and one-fifth of the exact cross sections, a result which is clearly to be expected given the rather anisotropic nature of the interaction potential. However, the qualitative shape of the excitation function is well reproduced for the three reactants vibrational levels studied, indicating that relative quantities, such as product energy distributions or branching ratios, might be well reproduced.

The QCT results are unexpectedly wrong. The origin of the discrepancies is traced back to the systematic violation of the ZPE conservation rule and the decisive importance of quantum effects for the present system. This causes reaction thresholds to be lower and the qualitative shape of the excitation function, for $v = 2$, to be strongly different. In addition, an unphysical queue which populates forbidden product rotational states is obtained in the product rotational distribution. Elimination of the unphysical trajectories ending below the products ZPE makes the QCT results qualitatively agree with the exact ones. However, the corrected QCT reactivity is systematically lower. This feature indicates, together with the structured pattern of the excitation function shape, that resonance formation is dominant in the reaction mechanism, even at high collision energies.

Acknowledgements

This work was partially supported by the Spanish Ministry of Science and Education (DGICYT Projects PB94-0909 and PB95-0598-C02-01) and the Generalitat de Catalunya (CUR Project 1996 SGR 000040). We also acknowledge the generous support of the "Centre de Supercomputació i Comuniacions de Catalunya (C4)" for the computer time allocated for this study. F.H.-L. thanks the Generalitat de Catalunya for a FPI research fellowship.

References

1 G. C. Schatz and M. A. Ratner, *Quantum Mechanics in Chemistry*, Prentice-Hall, Englewood Cliffs, NJ, 1993.
2 *J. Chem. Soc., Faraday Trans.*, 1997, **93**(5), *Dynamics of Molecules and Chemical Reactions*, ed. R. E. Wyatt and J. Z. H. Zhang, Marcel Dekker, New York, 1996; *Advances in Molecular Vibrations and Collision Dynamics*, ed. J. M. Bowman, vols. IIA and IIB, JAI Press, Greenwich, CT, 1994.
3 J. M. Launay and M. LeDourneuf, *Chem. Phys. Lett.*, 1989, **163**, 178; J. M. Launay, in *Dynamical Processes in Molecular Physics*, ed. G. Delgado-Barrio, IOP, Bristol, 1993.
4 J. M. Launay and M. LeDourneuf, *Chem. Phys. Lett.*, 1990, **169**, 473; J. M. Launay, *Theor. Chim. Acta*, 1991, **79**, 183.
5 P. Honvault and J. M. Launay, *Chem. Phys. Lett.*, 1998, **287**, 270.
6 (*a*) B. Lepetit and J. M. Launay, *J. Chem. Phys.*, 1991, **95**, 5159; (*b*) J. M. Launay and M. LeDourneuf, in *Physics of Electronic and Atomic Collisions*, Proceedings of the ICPEAC XVII, Brisbane, July 1991, Section 15, IOP Publishing, Bristol, 1992, p. 549.
7 J. M. Launay and S. B. Padkjaer, *Chem. Phys. Lett.*, 1991, **181**, 95.
8 S. E. Branchett, S. B. Padkjaer and J. M Launay, *Chem. Phys. Lett.*, 1993, **208**, 523.
9 F. S. Klein and L. Friedman, *J. Chem. Phys.*, 1964, **41**, 1789.
10 W. A. Chupka and M. E. Russell, *J. Chem. Phys.*, 1968, **49**, 5426.
11 K. R. Ryan and I. G. Graham, *J. Chem. Phys.*, 1973, **59**, 4260.
12 D. Van Pijkeren, J. Van Eck and A. Niehaus, *Chem. Phys. Lett.*, 1983, **96**, 20.
13 R. M. Bilotta and J. M. Farrar, *J. Chem. Phys.*, 1981, **75**, 1776.
14 Z. Herman and I. Koyano, *J. Chem. Soc., Faraday Trans. 2*, 1987, **83**, 127.
15 B. Brunetti, S. Falcinelli, A. Sassara, J. De Andrés and F. Vecchiocattivi, *Chem. Phys.*, 1996, **209**, 205.
16 J. B. A. Mitchell, in *1995 Workshop on dissociative recombination: theory, experiments and applications. III*, ed. D. Zajfman, J. B. A. Mitchell, D. Schwalm and B. R. Rowe, World Scientific, London, 1995, p. 21.
17 R. D. Mclaughlin and D. L. Thompson, *J. Chem. Phys.*, 1979, **70**, 2748.
18 T. Joseph and N. Sathyamurthy, *J. Chem. Phys.*, 1987, **86**, 704.
19 A. Aguado and M. Paniagua, *J. Chem. Phys.*, 1992, **96**, 1265.
20 J. Urban, R. Jaquet and V. Staemmler, *Int. J. Quantum Chem.*, 1990, **38**, 339.
21 J. Urban, L. Klimo, V. Staemmler and R. Jacquet, *Z. Phys. D*, 1991, **21**, 329.
22 P. Pendergast, J. M. Heck, E. F. Hayes and R. Jaquet, *J. Chem. Phys. Phys.*, 1993, **98**, 4543.
23 J. D. Kress, *Chem. Phys. Lett.*, 1991, **179**, 510.
24 J. D. Kress, *J. Chem. Phys.*, 1992, **95**, 8673.
25 J. D. Kress, R. B. Walker, E. F. Hayes and P. Pendergast, *J. Chem. Phys.*, 1994, **100**, 2728.
26 M. González, R. M. Blasco, X. Giménez and A. Aguilar, *Chem. Phys.*, 1996, **209**, 355.
27 C. Stroud and L. M. Raff, *Chem. Phys.*, 1980, **46**, 313.
28 E. F. Hayes, A. K. Q. Siu, F. M. Chapman, Jr. and R. L. Matcha, *J. Chem. Phys.*, 1976, **65**, 1901.
29 M. Gilibert, R. M. Blasco, M. González, X. Giménez, A. Aguilar, I. Last and M. Baer, *J. Phys. Chem. A*, 1997, **101**, 6822.
30 B. R. Johnson, *J. Comput. Phys.*, 1973, **13**, 445.
31 D. E. Manolopoulos, *J. Chem. Phys.*, 1986, **85**, 6425.
32 M. Gilibert, X. Giménez, F. Huarte-Larrañaga, M. González, A. Aguilar, I. Last and M. Baer, *J. Chem. Phys.*, in press.
33 F. J. Aoiz, L. Bañares and V. J. Herrero, *J. Chem. Soc., Faraday Trans.*, 1998, **94**, 2483.
34 M. Baer, I. Last and H. J. Loesch, *J. Chem. Phys.*, 1994, **101**, 9648, and references therein.
35 G. C. Schatz, in *The Theory of Chemical Reaction Dynamics*, ed. D. C. Clary, NATO ASI Series C, vol. 170, Reidel, Dordrecht, 1986, p. 1; G. C. Schatz, *Chem. Phys. Lett.*, 1983, **94**, 183.
36 H. Szichman, A. J. C. Varandas and M. Baer, *J. Chem. Phys.*, 1995, **102**, 3474.
37 X. Giménez, J. M. Lucas, A. Aguilar and A. Laganà, *J. Phys. Chem.*, 1993, **97**, 8578.
38 M. Gilibert, X. Giménez, M. González, R. Sayós and A. Aguilar, *Chem. Phys.*, 1995, **191**, 1.
39 A. Aguilar, M. Alberti, X. Giménez, X. Grande and A. Laganà, *Chem. Phys. Lett.*, 1995, **223**, 201.
40 A. Aguilar, M. Gilibert, X. Giménez, M. González and R. Sayós, *J. Chem. Phys.*, 1995, **103**, 4496.
41 A. Laganà, G. Ochoa de Aspuru, A. Aguilar, X. Giménez and J. M. Lucas, *J. Phys. Chem.*, 1995, **99**, 11696.
42 See, for instance, *Resonances in Electron–Molecule Scattering, van der Waals complexes and Reactive Chemical Dynamics*, ed. D. G. Truhlar, American Chemical Society, Washington DC, 1984.
43 M. Gilibert, M. González and R. Sayós, TRIQCT Program, 1992.
44 D. G. Truhlar and J. T. Muckerman, in *Atom–Molecule Collision Theory*, ed. R. B. Bernstein, Plenum Press, New York, 1981, p. 505, and references therein.
45 M. Ben Nun and R. D. Levine, *J. Chem. Phys.*, 1996, **105**, 8136, and references therein.
46 A. González-Ureña, personal communication; D. Bassi, personal communication.
47 G. C. Schatz, D. Sokolovski and J. N. L. Connor, *J. Chem. Phys.*, 1991, **94**, 4311.
48 J. M. Bowman, *Adv. Chem. Phys.*, 1985, **61**, 115; Q. Sun, J. M. Bowman, G. C. Schatz, J. R. Sharp and J. N. L. Connor, *J. Chem. Phys.*, 1990, **92**, 1677.

Paper 8/008552H

9.2 Fine structure details in cross-section and rotational distribution energy dependence for the $Ne + H_2^+ \rightarrow NeH^+ + H$ reaction.

Fermín Huarte-Larrañaga, Xavier Giménez, Josep M. Lucas and Antonio Aguilar
Departament de Química Física, Universitat de Barcelona
and Centre de Recerca en Química Teòrica, Universitat de Barcelona.
Jean-Michel Launay
PALMS, UMR 6627 du CNRS, Université de Rennes.

Abstract

Detailed energy dependences of state-to-state and state-to-all integral cross sections and product rotational distributions have been studied with exact 3D hyperspherical calculations for the $Ne + H_2^+ \rightarrow NeH^+ + H$ reaction. This analysis is motivated by the complex-forming nature of the title reaction, so that an structured behaviour is expected to be found. Results confirm the expectations. Integral cross sections show a marked structure as a function of energy. This structure has been characterized analyzing the state-to-state contributions, on one hand, and the evolution of the partial cross section cumulative sums as a function of total angular momentum, on the other. As expected, the key fact is that the strongly bound metastable states lead to peaks in the above quantities narrow enough to avoid an effective quenching of the resulting structure, when summing either over angular momentum or over final product states. This feature, which has already been found for other complex-forming reactions, indicates that quantum effects can be more relevant than expected, so as to require their explicit consideration when accurately characterizing a reactive event.

Introduction

Intense work has been devoted recently to the exact calculation of moderately involved three-atom systems' dynamics, mainly because of the availability of quantum reactive scattering methods capable of handling the associated computational requirements[1]. Besides representing a harder challenge from both the computational and methodological points of view, the exact calculation of involved systems dynamics has evidenced the quantum mechanical nature of several dynamical features in such an intense way that new intrinsic information has been generated. Perhaps the most relevant new feature is the dominant role played by metastable states and its influence on potentially measurable dynamical quantities. These metastable states can originate on a purely dynamical basis or, alternatively, may be formed by means of a mixed contribution, from an electronic minimum in the strong interaction region of the potential energy surface (PES) and a dynamical trapping owing to the existence of effective potential barriers. Several recent examples have appeared in the literature, demonstrating that the latter case leads to a dense spectrum of rather long lived metastable states[2,3]. These states, as it is well-known, appear as sharp peaks in the state-to-state fixed

total angular momentum reactive probability as a function of total energy. However, the fingerprints of the resonance pattern rarely survive when adequately summing and averaging the reaction probabilities over product states and partial waves, and are easily smoothed out. This is not case, instead, for the title system where, in particular, the structured behaviour of the reaction probability is not completely quenched. Even in some cases it leads to several, wider peaks which are more intense. Moreover, the large density of metastable states raises the whole integral cross section profile to larger values. This has caused, for this system, a large disagreement between quantum and classical calculations even in the high energy limit[4-6].

A preliminary account of these effects has been reported by some of the authors recently[4,5], on the title reaction. A CS-NIP method was used to calculate the state-to-all integral cross section over a fine energy grid. Results showed that: a) a dense spectrum of resonance peaks was found to dominate the reactivity over the whole energy range, b) important discrepancies were detected between the quantum method and the results of equivalent quasiclassical (QCT) calculations. In particular, the QCT reactivity was found to be only half of the quantum at 1.1 eV, the highest total energy considered. Another important disagreement was found at the threshold region, for the initial reactant vibrational level $v = 2$, but this was easily attributed to the inability of the QCT method to handle correctly the zero-point energy (ZPE) at threshold energies.

Such discrepancies suggested the application of an accurate method in order to confirm the above results, since as the reaction was dominated by complex collisions, this may impose severe limitations on the applicability of the centrifugal sudden approximation. A first stage consisted in generating exact cross sections over a coarse grid, covering the complete energy range chosen for the previous studies, in order to establish the global performance of the CS approach versus the exact one[6]. These results were encouraging, since little discrepancy was found. Consequently, it was argued that the importance of metastable states was not an artifact of the centrifugal approximation (usually, approximate methods lead to stronger resonance behaviours than more accurate ones), but could actually correspond to a true dynamical effect.

The above results motivated the present work. This has consisted on a fine energy grid study of the $Ne + H_2^+$ system, using the same PES as in previous studies, focusing mainly on state-to-state and state-to-all integral cross sections and product rotational distributions (PRD). The effect of the summation over partial waves, which accounts for the influence of angular momentum, will be obtained by evaluating the partial cumulative cross section sums for each value of the total angular momentum J. Special attention is paid on product rotational distributions and their variation with energy, since they are quantities amenable of experimental detection. For direct reactions, DRPs usually evolve smoothly with energy. In the present case, we expect to find, instead, more drastic variations with small changes in energy which, although being based on a relative measure, should be important enough. This would provide an additional way of detecting the influence of reactive scattering resonances, which is based on a relative rather than on an absolute measure of the total particle flux emerging in a given state.

The remainder of the paper is organized as follows. Results and the resulting discussion are presented on section II, which follow from a brief discussion of the details

of the calculation. Discussion focuses on the components of the total integral cross section in terms of product states and total angular momentum partial waves. Finally, section III concludes.

II. Outline of the calculations, results and discussion.

The method used in the present work is the close-coupling hyperspherical method of Launay and LeDourneuf, which has been described with detail elsewhere[7-9]. For this reason, only details concerning the actual calculation will be given here. Calculations have been performed on a dense energy grid essentially divided in two intervals, one with a total of 110 equally spaced points in the 0.698 - 0.800 eV range, and another from 0.8 eV to 1.1 eV with a cross section calculation every tenth of an electronvolt. For all energy values, converged integral cross sections have been computed. This meant including all relevant total angular momentum partial waves. Depending on the energy range, the number of partial waves was, approximately, 25, 35, 50 and 60 for 0.75, 0.80, 0.90 and 1.1 eV, respectively. For each partial wave, it has been seen, as common to previous calculations using the same method, that not all projections of total angular momentum (denoted as Ω) onto the quantization axis had to be included. In particular, all Ω's have been taken for $J < 7$ but $\Omega_{max} = 6$ for $J \geq 7$. This parameter was checked taking $\Omega_{max} = 10$ in several reactive probability calculations. Discrepancies were smaller than 1%. Actually, all calculations have been performed employing the internal basis obtained for this latter case, although using the smaller projection $\Omega_{max} = 6$. The remainder numerical parameters have been chosen to be the same as those discussed in the previous work on this system[6].

The strongly structured behaviour of the dynamics of the title reaction as a function of the total energy was previously anticipated when computing the $J = 0$ reaction probability. Figure 9.1 reproduces these results for the sake of completeness. From the average width of the probability peaks, a lifetime of roughly 1 ps. can be inferred for several of them, being in addition much more dense than for the related $He + H_2^+$ system[10,11].

Our main focus has been however to ascertain whether the prominent structure found for $J = 0$ might survive the angular momentum summation. Figure 9.2 shows the results corresponding to the integral, state-to-all cross sections as a function of total energy. It can be clearly seen that, in some of the cases, specially for initial $v = 2$ and the finely scanned energy range (from threshold to 0.8 eV), the structure is even more intense rather than being quenched. Cross sections for $v = 0$ and $v = 1$ show also a comparable structure, but since it is relative to the absolute value of the cross section, appears much smoother as a consequence of the y-axis scale. Returning to the $v = 2$ case, it is remarkable that oscillations around 0.75 eV are about $5\mathring{A}^2$, intense enough to consider it detectable with the high-resolution molecular beams apparatuses currently available[12].

The fact that the resonant structure survives the angular momentum summation is a rather new one. Previous calculations of integral cross sections for systems like

$H + H_2$, $F + H_2$ and $Cl + H_2$ and their isotopic variants[11] showed just the opposite behaviour, the complete quenching of the $J = 0$ structure, which was nevertheless less prominent. A first indication of the possibility of observing a surviving structure was given by Launay and LeDourneuf in their detailed calculations on the $He + H_2^+$ system[11], which showed how the existence of an electronic minimum in the PES leads to metastable states strongly bounded, so that the resulting peaks are narrow enough to avoid quenching on summation over J. An additional proof for such a behaviour has been recently provided by Russell and Manolopoulos[2], with their time-dependent wavepacket calculations for the $N^+ + H_2$ system. However, for this latter case the authors use the adiabatic rotational approximation to compute the integral cross sections. Then, in this case the conclusions should not be strictly definite, although they point again towards the survival of the resonant structure.

A detailed image of the angular momentum summation process can be obtained by computing the partial cumulative summations over J, i.e. an ensemble of curves each one containing the partial wave summation of the cross section until the J value labeling the curve. The resulting graph is shown in figure 9.3 for the initial $v = 2$, i.e. the case showing the most prominent structure. The partial summations are shown in steps of 5, except for the 40, 50 and 60 traces. Most interesting is the finer scanned range, since it shows several important features.

Firstly, it is important to notice that the $2J + 1$ factor premultiplying the reaction probability leads to a magnification of the contribution of the highest angular momenta. Most of the structure surviving the complete summation actually originates from the high-J contributions. This case corresponds to the structure around 0.75 eV.

A second case we distinguish corresponds to the peaks which are found in the entire J range, as it is seen approximately at 0.73 eV. This peak is found to exist even for $J = 0$ (that reaching a probability of 0.5 in the $v = 2$ case of figure 9.1), being subsequently amplified as larger J values are considered. It is remarkable that the peak position slightly shifts towards larger energy values as larger J's are considered. This fact is a clear indicator of an energy shifting owing to an increase in the effective potential barrier as a consequence of the larger centrifugal term. Perhaps a key feature would be that the shift caused by increasing J is small in this case, thanks to a relatively small rotational constant as a consequence of the Ne heavy mass (this is specially true when comparing with the $He + H_2^+$ case). Nevertheless, the survival conditions undoubtedly originate from the specially intense resonant peak found in the $J = 0$ probability profile, indicating a rather strongly bound metastable state.

A third feature we wish to stress is the approximate regularity in the shoulders (rather than peaks) appearing in the post threshold region, superimposed on the rapid increase of the integral cross section. A total of 7 almost equally spaced "bumps" can be easily identified in the integral cross section profile, both in figures 9.2 and 9.3. Those corresponding to larger energies show their corresponding component at smaller J's, as it is seen in figure 9.3 (so that they belong to the second case).

An opposite case, concerning the survival after J summation, is found for the three intense peaks appearing in the $J = 0$ probability, between 0.75 and 0.77 eV. The corresponding analysis for larger J's shows that they are clearly quenched already at the very first partial waves. It is seen however that those peaks, although being intense,

are much broader than the intense, sharp peak analyzed in the second case. These are clearly the conditions for an effective quenching on averaging with J, and, in addition, a larger contribution of direct reactivity could be found also in this case.

Another interesting issue to be analyzed is the possible influence of complex formation in those quantities referring to product states, like product energy distributions. This would lead to additional possibilities as far as the experimental detection of resonance features is concerned. For the present case, only product rotational distributions are relevant, since only one (and two in the high energy regime) product vibrational state remains open at the energies of the present study and, in particular, at the range scanned in detail. The consideration of product rotational distributions leads us to the state-to-state quantities. State-to-state integral cross sections as a function of total energy are shown in figure 9.4, for $v = 2$ again. Inspection of this figure allows to easily identify the product rotational thresholds. Once each product rotational channel is open, its state-to-state cross section shows a rather irregular behaviour. In particular, most of the rotational levels show an initial cross section increase, followed by a smooth decrease. Superimposed on it, a prominent structure is seen reflecting the influence of the resonance states. Some of the resonant structure appears correlated between several product rotational levels, in the sense that a peak in one particular rotational level appears at the same position of a dip associated with another rotational level.

Given the structured behaviour observed in the state-to-state integral cross section, it is hoped that strong variations are to be observed in the product rotational distributions with small changes in the total energy. An illustration for this is displayed in figure 9.5, where it is shown the product rotational distributions at four, closely spaced energies. In particular, the two first distributions, at 0.748 and 0.749 eV, differ by only 1 meV but change the maximum in the distribution from $j' = 1$ to $j' = 2$. Given the minor amount of increase in energy, we think this behaviour to be a rather remarkable one. The third and fourth cases, corresponding to energies of 0.755 and 0.757 eV show a much similar behaviour, although the highest in energy is slightly hotter that the lower. The decrease in population for the $j' = 2$ level is however more important, between the first and second group of transitions, since the overall energy difference is only 9 meV. A similar observation can be made for the decrease in the $j' = 0$ population, although it is not as intense as in the former case.

III. Conclusions

A detailed exploration of the energy dependence of integral state-to-state and state-to-all cross sections and product rotational distributions has been performed for the $Ne + H_2^+ \rightarrow NeH^+ + H$ reaction, on the same potential energy surface as previous studies.

The most remarkable feature is the strongly structured behaviour of all cross sections, and specially that corresponding to initial $v = 2$, reflecting the influence of metastable states. These states, originating from a mixed contribution of an electronic minimum and centrifugal barrier effective potentials, are bounded enough to show large lifetimes. The corresponding sharp probability peaks are found to survive the angular momentum summation.

However, the final structure which is present in the cross section stems from, basically, to kinds of behaviours. On one hand, most of the structure originates with the high angular momenta, i.e. it is magnified by the $2J + 1$ term appearing in the cross section expression. On the other, some peaks really survive the whole angular momentum summation since they manifest along the whole angular momentum range. This is the case of only specially intense and sharp peaks $J = 0$. In this case it is clear also how the centrifugal barrier shifts to higher energy values the peak position, as one consider higher angular momentum quantum numbers. The relatively small value of the rotational constant, owing to the heavy Ne mass, helps in avoiding the effective quenching of the peak, since it is little shifted.

Some of the structure, in particular that peaking between 0.73 and 0.77 eV, approximately, for $v = 2$, is prominent enough to be amenable for experimental detection in high-resolution molecular beams machines[12]. The possibility of experimental detection through relative, in opposite to absolute, measurements has also been explored by computing the state-to-state integral cross sections and the related product rotational distributions. Relevant variations in the latter quantity are found with very small increases in total energy. This important variation could be used as an additional indicator of the presence of reaction complexes during the collision. Of course, the final word has to be said once available the experimental data and improved estimations of the potential energy surface.

Acknowledgements

The authors wish to thank the Spanish DGCYT (grants PB97-0919 and PB95-0598-C02-01) and the Generalitat de Catalunya (CUR grant 1998SGR-00008). One of us (F.H.L.) gratefully acknowledges a predoctoral fellowship from the Catalan CIRIT. Computer time has been generously allocated by the Centre de Computació i Comunicacions de Catalunya (C4).

References

1 Faraday Discussions of the Chemical Society. Issue on "Chemical Reaction Theory", 110 (1998).

2 C.L. Russell and D. E. Manolopoulos, J. Chem. Phys. 110 (1999) 177.

3 Y.C. Zhang, L.X. Zhan, Q.G. Zhang, W. Zhu and J.Z.H. Zhang, Chem. Phys. Lett. 300 (1999) 27.

4 M. Gilibert, R.M. Blasco, M. Gonzalez, X. Giménez, A. Aguilar, I. Last and M. Baer, J. Phys. Chem. A 101 (1997) 6822.

5 M. Gilibert, X. Giménez, F. Huarte-Larrañaga, M. González, A. Aguilar, I. Last and M. Baer, J. Chem. Phys. 110 (1999) 6278.

6 F. Huarte-Larrañaga, X. Giménez, J.M. Lucas, A. Aguilar and J.M. Launay, Phys. Chem. Chem. Phys. 1 (1999) 1125.

7 J.M. Launay and M. LeDourneuf, Chem. Phys. Lett. 163 (1989) 178.

8 P. Hovault and J.M. Launay, Chem. Phys. Lett. 287 (1998) 270.

9 P. Honvault and J.M. Launay, Chem. Phys. Lett. 303 (1999) 657.

10 B. Lepetit and J.M. Launay, J. Chem. Phys. 95 (1991) 5159.

11 J.M. Launay and M. LeDourneuf, in Physics of Electronic and Atomic Collisions, Proceedings of the ICPEAC XVII, Brisbane, July 1991, Section 15, IOP Publishing, Bristol, 1992, p. 549.

12 A. Gonzalez Ureña, personal communication. D. Bassi, personal communication.

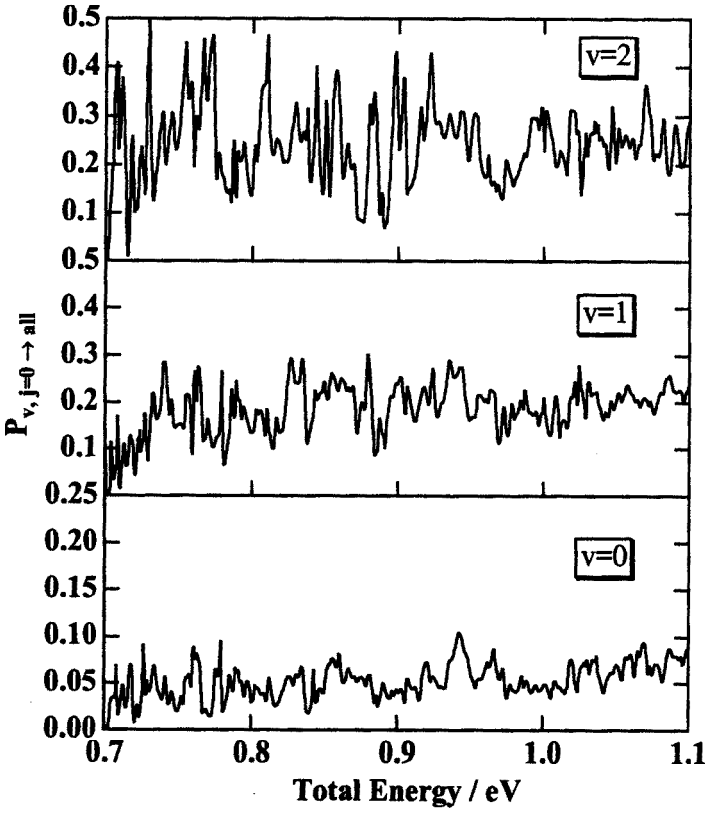

Figure 9.1: State-to-all $J = 0$ reaction probability as a function of total energy, for the first three reactant vibrational levels.

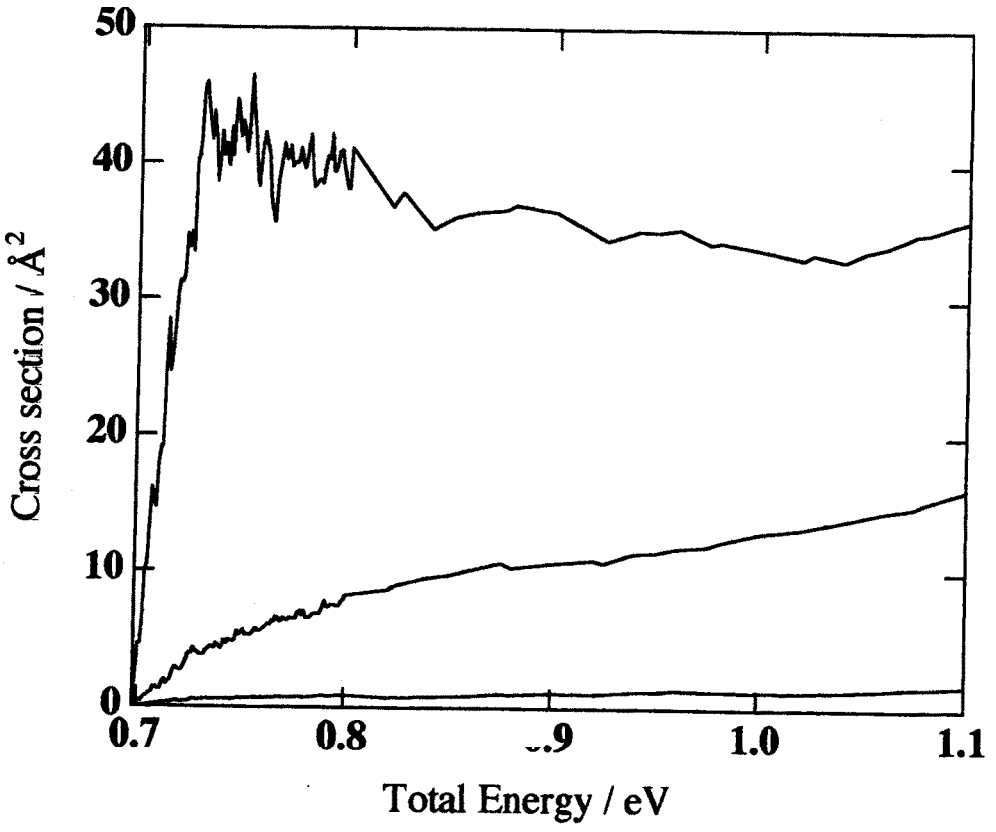

Figure 9.2: State-to-all integral cross section as a function of total energy, for the first three reactant vibrational levels.

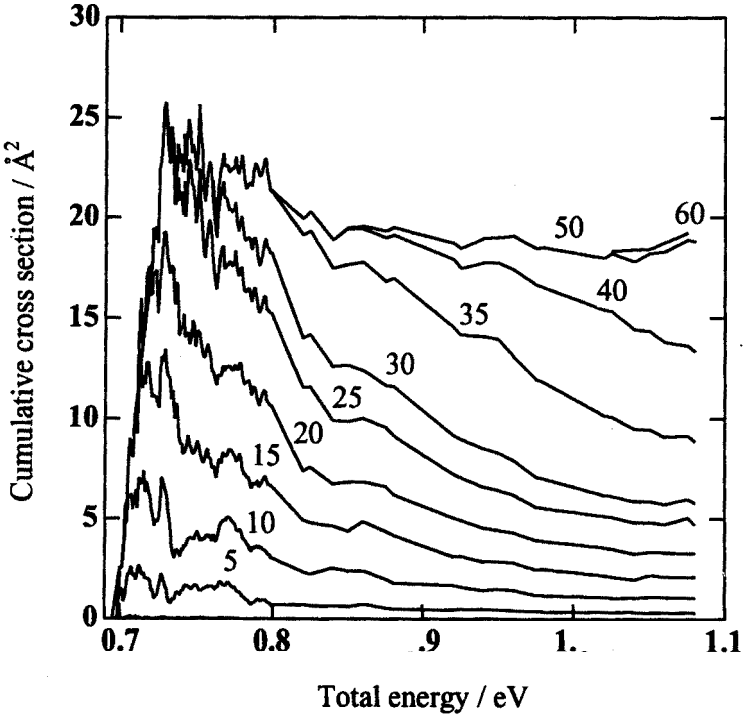

Figure 9.3: Cumulative cross section dependence as a function of total energy, for several values of the total angular momentum and initial reactant vibrational level $v = 2$. Each trace is labeled by the maximum total angular momentum quantum number value included in the partial cross section summation.

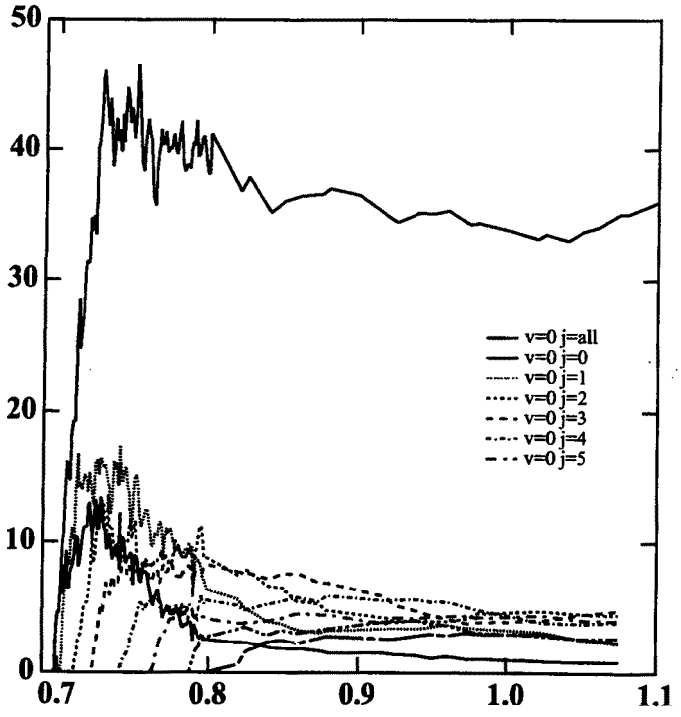

Figure 9.4: State-to-state integral cross sections, for several values of the product rotational angular momentum quantum number, for initial $v = 2$, as a function of total energy. The state-to-all integral cross section for $v = 2$ has been also included for completeness.

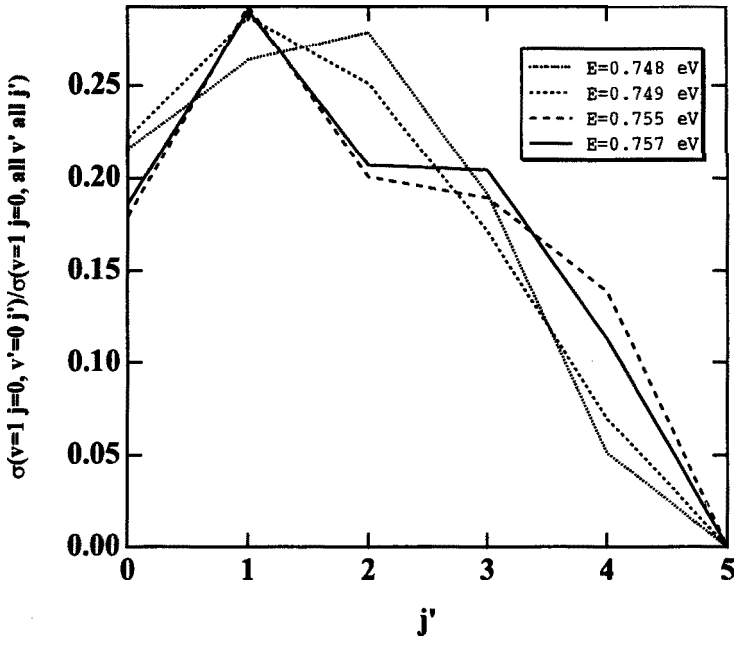

Figure 9.5: Product rotational distribution, at four selected total energies, for initial v = 1. All distributions have been normalized to its corresponding sum.

Appendix A

Calculation of Inelastic scattering S-matrix elements.

The close coupling equations have to be integrated outwards in the scattering coordinate (r in our case) from a small enough value of r so that all components of the wavefunction can be taken as zero, to a value where the potential can be neglected and we there have the asymptotic solution in terms of the free particle functions:

$$\psi(r) \sim e^{\mathbf{ikr}}\mathbf{A} + e^{-\mathbf{ikr}}\mathbf{B} \tag{A.1}$$

where $\mathbf{k}$ is the diagonal matrix of wave vectors k_i. This expression is only valid for the collinear case of section 2.6, for the three-dimensional case one should use $e^{(\mathbf{ikr}-\ell\pi/2)}$ instead of $e^{\mathbf{ikr}}$.

The coefficients, here expressed in matrix notation as $\mathbf{A}$ and $\mathbf{B}$, are square matrices whose dimension equals the number of channels included in the total wavefunction expansion, whether closed or open. To obtain the Scattering matrix one must transform A.1 so that the exponentially growing terms are zero for closed channels.

Let's start by partitioning the coefficient matrices into open and closed blocks:

$$\mathbf{A} = \begin{vmatrix} \mathbf{A}_{OO} & \mathbf{A}_{OC} \\ \mathbf{A}_{CO} & \mathbf{A}_{CC} \end{vmatrix}, \quad \begin{vmatrix} \mathbf{B}_{OO} & \mathbf{B}_{OC} \\ \mathbf{B}_{CO} & \mathbf{B}_{CC} \end{vmatrix} \tag{A.2}$$

For the $\mathbf{B}$ matrix, that multiplying the exponentially growing term, a transformation can be written that leaves only the open-open elements non zero:

$$\begin{bmatrix} \mathbf{B}_{OO} & \mathbf{B}_{OC} \\ \mathbf{B}_{CO} & \mathbf{B}_{CC} \end{bmatrix} \begin{bmatrix} \mathbf{I} & 0 \\ \mathbf{\Gamma} & 0 \end{bmatrix} = \begin{bmatrix} \mathbf{B}'_{OO} & 0 \\ 0 & 0 \end{bmatrix} \tag{A.3}$$

which requires $\mathbf{\Gamma} = -\mathbf{B}_{CC}^{-1}\mathbf{B}_{CO}$ and consequently the new open-open subblock becomes:

$$\mathbf{B}'_{OO} = \mathbf{B}_{OO} - \mathbf{B}_{OC}\mathbf{B}_{CC}^{-1}\mathbf{B}_{CO} \tag{A.4}$$

The same transformation has to be applied on the $\mathbf{A}$ matrix and gives an open-open submatrix which is

$$\mathbf{A}'_{OO} = \mathbf{A}_{OO} - \mathbf{A}_{OC}\mathbf{B}_{CC}^{-1}\mathbf{B}_{CO} \tag{A.5}$$

Once we have ensured that submatrices of **B** will be zero for closed channels, still remains to transform $\mathbf{A}'$ so that all incoming waves are in pure internal states. A further transformation is then carried away to make coefficients of e^{ikr} unity, this involves pre-multiplication of both open-open subblocks by $(A'_{OO})^{-1}$. The resulting matrix for the open channels becomes:

$$\mathbf{B}''_{OO} = \left(\mathbf{B}_{OO} - \mathbf{B}_{OC}\mathbf{B}_{CC}^{-1}\mathbf{B}_{CO}\right)\left(\mathbf{A}_{OO} - \mathbf{A}_{OC}\mathbf{B}_{CC}^{-1}\mathbf{B}_{CO}\right)^{-1} \tag{A.6}$$

Thus, the asymptotic form of the wavefunctions for the open channels is therefore of the following form:

$$\psi(r) \sim e^{ikr} + e^{-ikr}\mathbf{B}''_{OO} \tag{A.7}$$

Comparing this expression with 2.67 one can obtain the S-matrix elements in terms of the previous coefficients

$$S_{ij} = -\left(\frac{k_i}{k_j}\right)^{1/2} B''_{ij} \tag{A.8}$$

Appendix B

The Partitioning Technique

One of the most elegant ways of proving the dimensionality reduction achieved by the optical potential is following the so-called *partitioning technique*. This technique was initially applied in the field of Nuclear Physics[5] and soon was adopted for the study of molecular systems in the middle 60s[24]. The idea underlying on this method is that, through paying attention to the component of the wavefunction that might be of interest, one can obtain an *exact* equation for this component if the actual potential is replaced by an equivalent one.

The partitioning technique consists, thus, in the introduction of two projection operators $\hat{P}$ and $\hat{Q}$ defined by the following properties:

$$\hat{P} + \hat{Q} = \hat{I} \tag{B.1}$$

$$\hat{P}^2 = \hat{P} = \hat{P}^\dagger \tag{B.2}$$

so that

$$\hat{P}\hat{Q} = 0 \tag{B.3}$$

and $\hat{P}\psi$ yields the wavefunction component in which we are interested. Using property B.1 in the Schrödinger equation , we can write the equation formally as two coupled equations in terms of the $\hat{P}$ and $\hat{Q}$:

$$\hat{P}\left(\hat{H} - E\right)\hat{P}\psi = -\hat{P}\hat{H}\psi \tag{B.4}$$

$$\hat{Q}\left(\hat{H} - E\right)\hat{Q}\psi = -\hat{Q}\hat{H}\psi \tag{B.5}$$

$$\tag{B.6}$$

where the two unknown functions are then $\hat{P}\psi$ and $\hat{Q}\psi$. This is known as well as the *Feshbach decomposition*. Existence of an effective potential that treats exactly the component in which we are interested can be proven isolating $\hat{Q}\psi$ in B.6, substituting the resulting expression in B.5 and taking into account properties B.1,B.2:

$$\left\{\hat{P}(\hat{H} - E)\hat{P} + \hat{P}(\hat{H} - E)\hat{Q}[\hat{Q}(E - \hat{H})\hat{Q}]^{-1}\hat{Q}(\hat{H} - E)\hat{P}\right\}\hat{P}\psi = 0 \tag{B.7}$$

One can express abreviately the latter expression as:

$$\left\{\hat{P}(\hat{H} - E)\hat{P} + V_{opt}\right\}\hat{P}\psi = 0 \tag{B.8}$$

where the *exact optical potential*, V_{opt}, is

$$V_{opt} = \hat{Q}(E - \hat{H})\hat{Q}]^{-1}\hat{Q}(\hat{H} - E)\hat{P} \tag{B.9}$$

This potential would thus represent the function that allows us to have a projection $\hat{P}\psi$ of the total wavefunction *as if* we had solved the whole problem. More explicitly, the projection is usually written as:

$$\hat{P} = \sum_{i=1}^{N} |\phi_i >< \phi_i| \tag{B.10}$$

so that N determines how large is the space onto which $\hat{P}$ projects, or, in our case, determines the number of states in the expansion 2.68.

Appendix C

Probability flux absorption by a NIP.

In this section, a proof will be given on how the introduction of an imaginary component in the potential associated to the equations of motion causes a loss or gain of probability flux in time independent problems. To do this, we will start from the quantum mechanical definition of probability current, i.e., the number of particles crossing a given area by unit time. If we consider the classical expression $\mathbf{j} = \rho\mathbf{v}$ and knowing that in the position representation the velocity is written as $\mathbf{v} = -\frac{i\hbar}{m}\nabla$, we can write the quantum mechanical expression for the flux as:

$$\mathbf{j} = \frac{\hbar}{2im}\left\{\psi^*\nabla\psi - \psi\nabla\psi^*\right\} \tag{C.1}$$

One then obtains the vector $\mathbf{j}$, in all space points, so that $\mathbf{j}d\mathbf{S}dt$ is the probability for a particle to cross an area element $d\mathbf{S}$ in a time dt. For a stationary system the flux, or probability current, must be conserved so one can establish that:

$$\nabla\mathbf{j} = 0 \tag{C.2}$$

Calculating the divergence of C.1 one finds:

$$\nabla\mathbf{j} = \frac{\hbar}{2im}\left\{\psi^*\nabla^2\psi - \psi\nabla^2\psi^*\right\} \tag{C.3}$$

since both ψ and ψ^* satisfy the Schrödinger equation the following relation:

$$\psi^*\nabla^2\psi = -\psi^*\frac{2m}{\hbar^2}(E - V)\psi = \psi\nabla^2\psi^* \tag{C.4}$$

implies that the divergence in C.3 is zero and therefore the flux is conserved.

Actually, the relation in C.4 is only valid when V is real. If we consider the possibility of V being complex, so that it can be written as $V = V_r \pm iV_i$, with V_r and V_i as real functions of the coordinates, then the left hand of C.4 reads

$$\psi^*\nabla^2\psi = -\psi^*\frac{2m}{\hbar^2}(E - V_r \mp iV_i)\psi \tag{C.5}$$

and the right hand correspondingly is

$$\psi\nabla^2\psi^* = -\psi\frac{2m}{\hbar^2}(E - V_r \pm iV_i)\psi^* \tag{C.6}$$

and therefore the flux divergence is written as:

$$\nabla \mathbf{j} = \mp\frac{2V_i\psi\psi^*}{\hbar} \tag{C.7}$$

for which the imaginary component of V renders a particle *absorption* at a rate proportional to $\alpha\rho$, where $\alpha = 2V_i/\hbar$ and $\rho = \psi\psi^*$ when $V_i < 0$ and a particle *generation* at the same rate when $V_i > 0$.

Given there is no connection between complex operators and physical observables, the use of these potentials can only be justified as a phenomenological approximation to the problem.

We would like to point out as well that the loss of flux conservation implies the loss of unitarity of the involved operators. This will turn out into variations to the commonly assumed equivalences between unitary matrices.

Appendix D

Primitive $\{\mathcal{Y}\}$ basis set.

In this section, an outline on the derivation of the $\{\mathcal{Y}\}$ primitive functions will be given. These functions serve as a basis set for the variational expansion in the solution of the ρ- and Ω- dependent Hamiltonian in the Hyperpsherical approach, as developed by Launay and LeDourneuf. Further deepening in the derivation of these functions has been published by the authors[35].

In the case of two identical atoms B and C, the solutions of equation 5.8 have to be expanded onto common eigenfunctions of three operators: $\Lambda_0^2 + 4\Omega^2/\sin^2\theta$, the inversion $\hat{I}$ and the permutation $\hat{P}$ of B and C: defined for the special case $\epsilon_P = +1$ (even permutation symmetry) by

$$\mathcal{Y}_{Kv}^{\epsilon_I \epsilon_P \Omega}(\overline{\omega}) = g_K^{v\Omega}(\theta) h^{\epsilon_P}(v\phi - \Omega\pi/2) \tag{D.1}$$

where $\epsilon_P = \pm 1$ is the permutation eigenvalue and v is a non-negative integer that is even when $\epsilon_I = +1$ and odd when $\epsilon_I = -1$.

$$h^{\epsilon_P}(x) = \begin{cases} \cos x & ; \quad \epsilon_P = +1 \\ \sin x & ; \quad \epsilon_P = -1 \end{cases} \tag{D.2}$$

The function $g_K^{v\Omega}$ is a solution of the one-dimensional equation

$$\left(-\frac{4}{sin2\theta} \frac{d}{d\theta} + \frac{v^2}{\cos^2\theta} + \frac{4\Omega^2}{\sin^2\theta} \right) g_K^{v\Omega}(\theta) = K(K+4) g_K^{v\Omega}(\theta) \tag{D.3}$$

with $K = v + 2\Omega + 4n$, n being a non-negative integer. These primitive functions are delocalized in configuration space, whereas the surface functions are more and more concentrated in the arrangement valleys around $(\theta = 0)$ as ρ increases. Consequently, the expansion of the φ_k functions on the $\mathcal{Y}$ basis converges slowly at large hyperspherical radius. Faster convergence can be achieved by using for large ρ a contracted basis, obtained by diagonalizing the representation of the operator $1/cos^2\theta$ in the $\mathcal{Y}$ and by keeping the states with eigenvalues smaller than a criterion, namely $1/cos^2\theta_\rho$. Here θ_ρ depends on ρ and on two given parameters ρ_0 and θ_0:

$$\sin\theta_\rho = \rho_0 \sin\theta_0 / \rho$$

The resulting eigenfunctions are localized in the interval $[0, \theta_\rho]$ and are the most useful to represent the surface states.

Equation D.3 has analytical solution in terms of Jacobi polynomials[33, 35]. However, the authors found it preferable to perform a further expansion to solve the equation, this time in terms of trigonometric functions:

$$g_K^{v\Omega}(\theta) = a_v(\theta) \sum_{k=0}^{[K/4]} b_k(\theta) c_{kK}^{v\Omega} \tag{D.4}$$

where,

$$\begin{cases} \Omega \text{ is even} & \begin{cases} b_k(\theta) = \cos 2k\theta & ; \ [v/2] \text{ is even} \\ b_k(\theta) = \cos(2k+1)\theta & ; \ [v/2] \text{ is odd} \end{cases} \\ \Omega \text{ is odd} & \begin{cases} b_k(\theta) = \sin(2k+1)\theta & ; \ [v/2] \text{ is even} \\ b_k(\theta) = \sin(2k+2)\theta & ; \ [v/2] \text{ is odd} \end{cases} \end{cases} \tag{D.5}$$

and

$$a_v(\theta) = \begin{cases} 1 & ; \ v \text{ is even} \\ \cos^{1/2}\theta & ; \ v \text{ is odd,} \end{cases} \tag{D.6}$$

where $[x]$ denotes the integer part of x. When $\Omega = 0$ it can be seen that the $\mathcal{Y}$ functions reduce to the $J = 0$ Smith-Whitten hyperspherical harmonics.

If one considers now the case of three different atoms, the potential is no longer invariant to the permutation of B and C and therefore the primitive basis must contain both parity functions $\epsilon = \pm 1$. On the other hand, the case of three identical atoms, it is the cyclic permutations that commutes with V.

The advantage of this trigonometric expansion is that it can simplify considerably the integrals of V. It can be seen that the size of the primitive basis set for each Ω is proportional to K_m^2 (maximum value of K included in D.4 and increases as ρ^2).

Bibliography

[1] L.D. Fadeev; *Mathematical Aspects of the Three-Body Problem* in *Quantum Scattering Theory*, Israel Program for Scientific Translations, Jerusalem, 1965.

[2] C.J. Joachain; *Quantum Collision Theory*, North-Holland, Amsterdam 1983.

[3] J.R. Taylor; *Scattering Theory*, Wiley and Sons, New York, 1972.

[4] J.N. Murrell and S.D. Bosanac; *Introduction to the Theory of Atomic and Molecular Collisions*, Wiley and Sons, New York, 1987.

[5] H. Feshbach; *Ann. Phys.* **1958**, 5, 357; **1962**, 19, 287.

[6] N.F. Mott, H.S.W Massey; *The theory of atomic collisions.* Oxford Univ. Press, London, 1969.

[7] T.F. George, J. Ross; *Annu. Rev. Phys. Chem.* **1974**, 24, 263.

[8] D.A. Micha; *Optical models in molecular collision theory*, in W.H. Miller (Ed.) *Dynamics of Molecular Collisions. Part A.* Plenum Press, New York, 1976. pp 81-129.

[9] D.A. Micha, *J. Chem. Phys.* **1969**, 50, 722.

[10] R.D. Levine, *J. Chem. Phys.* **1968**, 49, 51; **1969**, 50, 1.

[11] G. Wolken Jr., *J. Chem. Phys.* **1972**, 56, 2592.

[12] D.W. Schwenke, D. Thirumalai and D.G. Truhlar, *Phys. Rev. A* **1983**, 28, 3258.

[13] R. Marriot and D.A. Micha, *Phys. Rev.* **1969**, 180, 120.

[14] D. A. Micha and M. Rotenberg, *Chem. Phys. Lett* **1970**, 6, 79; **1971**, 11, 626.

[15] J.L.J. Rosenfeld and J. Ross, *J. Chem. Phys.* **1966**, 44, 188.
H.Y. Sun and J. Ross, *J. Chem. Phys.* **1967**, 46, 3306.
C. Nyeland and J. Ross, *J. Chem. Phys.* **1968**, 49, 843.
R.E. Roberts and J. Ross, *J. Chem. Phys.* **1970**, 52, 1464.

[16] R. Kosloff, D. Kosloff; *J. Comput. Phys.* **1986**, 63, 363.

[17] M. Baer, H.R. Mayne, V. Kahre, D.J. Kouri; *Chem Phys. Lett.* **1980**, 72, 269.

[18] D. Neuhauser and M. Baer, *J. Chem. Phys.* **1989**, 91, 4651.

[19] D. Neuhauser and M. Baer, *J. Chem. Phys.* **1990**, 92, 3419.

[20] T. Seideman and W.H. Miller, *J. Chem. Phys.* **1992**, 96, 4412; **1992**, 97,) 2499;
W.H. Miller,*Acc. Chem. Res.* **1993**, 26, 174;
U. Manthe and W.H. Miller, *J. Chem. Phys.* **1993**, 99, 3411.

[21] D. Hirst. *Potential Energy Surfaces. Molecular Structure & Reaction Dynamics.*, Taylor & Francis, London and Philadelphia, 1985.

[22] P. Honvault, J.M. Launay *Chem. Phys. Lett.* **1999**, 303, 657.

[23] C.J.G. Jacobi. *C. R. Acad. Sci.* **1842**, 15, 236.

[24] R.D. Levine; *Quantum mechanics of molecular rate processes.* Oxford Univ. Press, London, 1969.

[25] R.N. Zare; *Angular Momentum. Understanding Spatial Aspects in Chemistry and Physics*, Wiley and Sons, New York, 1988.

[26] X. Giménez; Tesi Doctoral, 1990, Universitat de Barcelona.

[27] V. Khare, D.J. Kouri, M. Baer; *J. Chem. Phys.* **1979**, 71, 1199.

[28] R.T. Pack, G.A. Parker *J. Chem. Phys.* **1987**, 87, 3888.

[29] Smith F. T. *J.Math. Phys.* **1962**, 3, 735.

[30] Whitten R.C. and Smith F.T. *J. Math. Phys.* **1968**, 9, 1103.

[31] Fock V. *Kgl Norske Videnskab Sclkabs Forh.* **1958**, 31, 138.

[32] Johnson B.R. *J. Chem. Phys.* **1980**, 73, 5051.

[33] de Fazio, D. *Doctoral Thesis* **1996**, Università di Perugia.

[34] V: Aquilanti, S. Cavalli, C. Colletti, D. deFazio and G. Grossi *Hyperlangular Momentum: Applications to atomic and molecular science.* from *New methods in Quantum Theory*; C. A. Tsipis, V.S. Popov, D.R: Herschbach, J.S. Avery, Eds. Kluwer, Dordrech, 1995.

[35] J.M Launay and M. Le Dorneuf *Chem. Phys. Let.* **1989**, 163, 178.

[36] F. Mrugala and D. Secrest, *J. Chem. Phys.* **1983** 78, 5954.

[37] B.R. Johnson *J. Comput. Phys.* **1973**, 13, 445.

[38] D.E. Manolopoulos *J. Chem. Phys.* **1986**, 85, 6425.

[39] F. Mrugala, *J. Comput. Phys.* **1985**, 58, 113.

[40] M.H. Alexander, G. Parlant, T. Hemmer. *J. Chem. Phys.*,**1989**, 91, 2388.

[41] D.E. Manolopoulos, Jamieson, Pradhan *J. Comput. Phys.* **1993**, 105, 169.

[42] D. Secrest *Rotational Excitation I: The Quantal treatment* in *Atom - Molecule collision theory. A guide for the experimentalist* Edited by R.B. Bernstein, Plenum Press, New York, 1979.

[43] D.J. Zvijac, J.C. Light, *Chem. Phys.* **1976**, 12, 237.

[44] J.C. Light, R.B. Walker, *J. Chem. Phys.* **1976**, 65, 4272.

[45] E.P. Wigner, K.T. Tang, *Phys. Rev.* **1947**, 72, 29.

[46] B.R. Johnson *J. Chem. Phys.* **1983**, 79, 1906, 1916.

[47] B. Lepetit, J.M. Launay, M. Le Dorneuf *Chem. Phys.* **1986**, 106, 103.

[48] J.M. Launay *Introduction to the quantum theory of reactive scattering* in *Dynamical Processes in Molecular Physics* edited by G. Delgado-Barrio, IOP, London, 1993.

[49] M. Gilibert, X. Giménez, F. Huarte-Larranaga, M. González, A. Aguilar, I. Last anb M. Baer, *J. Chem. Phys.* **1999**, 110, 6278.

[50] S.I. Drozdov, *JETP Lett.* **1955**, 1, 591.
D.M. Chase, *Phys. Rev.* **1956**, 104, 838.
K. Alder, A. Winther, *Mater. Fys. Medd. Dansk. Vidensk. Selsk.* **1960**, 32, 1.

[51] K. Takayanagi, *Prog. Theor. Phys. Suppl.* **1963**, 25, 1.
K.H. Kramer, R.B. Bernstein, *J. Chem. Phys.* **1964**, 40, 200.
R.J. Kross, D.R. Herschbach, *J. Chem. Phys.* **1965**, 43, 3530.
R.B: Bernstein, K.H. Kramer, *J. Chem. Phys.* **1966**, 44, 4473.
R.J. Kross Jr., *J. Chem. Phys.* **1967**, 46, 609.

[52] C.F. Curtiss, *J. Chem. Phys.* **1968**, 48, 1725; **1968**, 49, 1952.

[53] T.P. Tsien, R.T. Pack, *Chem. Phys. Lett.* **1970**, 6, 54.
T.P. Tsien, G.A. Parker, R.T. Pack, *J. Chem. Phys.* **1973**, 59, 5373.

[54] D.Secrest, *J. Chem. Phys.* **1970**, 62, 710.

[55] R.T. Pack, *J. Chem. Phys.* **1974**, 60, 633.

[56] J.M. Bowmann, K.T. Lee, *J. Chem. Phys.* **1978**, 68, 3940.

[57] V. Khare, D.J. Kouri, *J. Chem. Phys.* **1978**,69, 4916.

[58] A. Kuppermann, G.C. Schatz, M. Baer; *J. Chem. Phys.* **1976**, 65, 4596.

[59] A. Kuppermann, *Chem. Phys. Lett.* **1975**, 32, 374.

[60] G.D. Barg, G. Drohlshagen; *Chem. Phys.* **1980**, 47, 209.

[61] J.M. Bowmann, K.T. Lee, *J. Chem. Phys.* **1980**, 72, 5071.

[62] D.J. Kouri, V. Kahre, M. Baer, *J. Chem. Phys.* **1981**, 75, 1179.

[63] J.M. Bowmann, K.T. Lee, *Chem. Phys. Lett.* **1979**, 64, 291.

[64] M. Baer, V. Khare, D.J. Kouri, *Chem. Phys. Lett.* **1979**, 68, 378.

[65] D.C. Clary, G. Drolshagen, *J. Chem. Phys.* **1982**, 76, 5027.

[66] D.C. Clary, *Mol. Phys.* **1981**, 1067, 1083.

[67] D.C. Clary, *Chem. Phys.* **1983**, 81, 379.

[68] X. Giménez, J.M. Lucas, A. Aguilar and A. Laganà, *J. Phys. Chem.* **1993**, 97, 8578.
M. Gilibert, X. Giménez, M. González, R. Sayós and A. Aguilar, *Chem. Phys.* **1995**, 191, 1.
A. Aguilar, M. Albertí, X. Giménez, X. Grande and A. Laganà, *Chem. Phys. Lett.* **1995**, 233, 201.
A. Aguilar, M. Gilibert, X. Giménez, M. González and R. Sayós, *J. Chem. Phys.* **1995**, 103, 4496.
A. Laganà, G. Ochoa de Aspuru, A. Aguilar, X. Giménez and J.M. Lucas, *J. Phys. Chem.* **1995**, 99, 11696.
M. González, R.M. Blasco, X. Giménez and A. Aguilar, *Chem. Phys.* **1996**, 209, 355.
F. Huarte-Larrañaga, X. Giménez, M. Albertí , A. Aguilar, A. Laganà and J.M. Alvariño, *Chem. Phys. Lett.* **1998**, 282, 91.
F. Huarte-Larrañaga, X. Giménez, M. Albertí, A. Aguilar, A. Laganà and J.M. Alvariño, *Phys. Chem. Chem. Phys.* **1999**, 1, 1133.

[69] T. Peng, W. Zhu, D. Wang and J.H. Zhang *Faraday Discussion* **1998**, 110, 159.